Modelling a solar power tower external receiver in Engineering Equation Solver

Rita Sofia Feijão Almeida de Oliveira
rita.feijao@tecnico.ulisboa.pt

Instituto Superior Técnico, Universidade de Lisboa, Portugal
April 2017

Abstract

The solar tower system coupled with a thermal energy storage system using molten salts, has already been successfully demonstrated as capable of supplying electricity to the grid, even when solar radiation is not available. This work focuses on developing a computational model on EES capable of performing steady-state energy simulations for a molten salt based external tubular receiver for solar tower plants, hence addressing the need for detailed and steady-state simulation tools. The model is based on a one-dimensional simplified approach, since it considers the temperature at the external surface of the tubes to vary only on the axial direction, hence neglecting circumferential and radial variations of the calculated parameters on each tube that comprises the receiver. Also, the model neglects conduction through the tube´s wall in both directions and between neighboring tubes, since it has a low value when comparing to the heat flow rate on the horizontal direction. No experimental data was available to validate the model, therefore two simulations were performed and discussed by comparing the results with reference papers, when using the same inputs for incident flux density, geometrical parameters, heat transfer fluid and ambient conditions. It was concluded that the model is suitable for simulating the energy performance of the receiver, since it correctly estimates the final temperature of the working fluid. In this work, it was also developed a Gemasolar-type heliostat field model on the software Tonatiuh, useful for obtaining the distribution of the incident flux density on an external receiver for different solar angles.

Keywords: Solar power tower; external receiver; molten salt; energy performance; heliostat field.

1. Introduction

Concentrating Solar Power (CSP) stands side by side with wind power, hydro and photovoltaic technologies as a possible substitution for conventional technologies powered by fossil fuels and, as the world evolves towards a cleaner and more sustainable energy production, the development and optimization of this technology is a growing topic of research (EASAC, 2011). CSP plants have the potential to reach high temperatures of the working fluid, hence allowing for greater power cycle efficiencies (Neises & Wagner, 2012). Solar Power Tower (SPT) systems are suitable for utility-scale applications (in the 10 to 100 MWe range (Reilly, Hugh E. & Kolb, 2001)) and are developing rapidly around the world, so there is a potential cost reduction for this systems (Yao, Hu, & Gao, 2015). The motivation to do this work is aligned with the EU FP7 STAGE-STE project, particularly the development of CSP plant performance models to analyse the technical and economic performance of CSP+D plants. This work is within the technology objectives of the project, as it supplies a tool able of predicting the external receiver performance, further allowing system optimization and economic benefits.

The primary reason for developing a model of a SPT external tubular receiver was to provide a tool capable of assisting the user on the simulation of the solar-derived energy that a system can supply to the working fluid, on a steady-state condition. The model was developed for the application on a SPT external receiver that uses molten salt as Heat Transfer Fluid (HTF) and with a conventional Rankine cycle as the power conversion system.

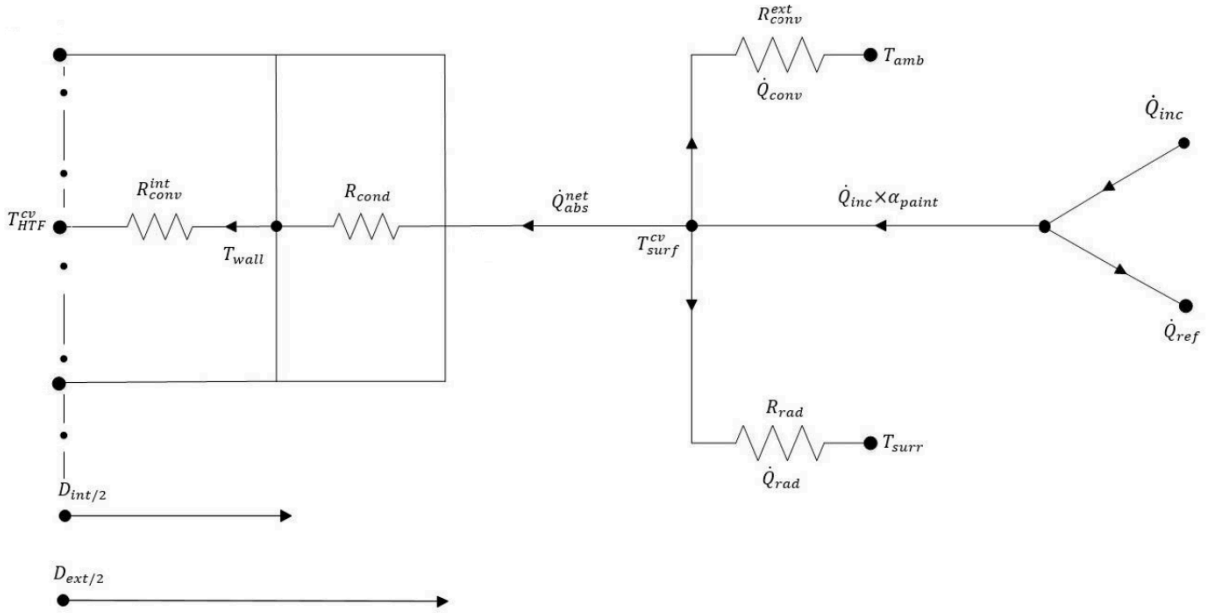

Figure 1 – Thermal model presented on the receiver tube section.

The model can calculate, in detail, all the thermal exchanges that occur during the transfer of energy to the HTF, with the final output being the temperature of the HTF leaving the receiver and the external surface temperature of the receiver. Each tube, in each panel of the receiver, is discretized in a certain number of control volumes (CV) and the energy balance allows obtaining the temperature increase in each point depending on the respective incident irradiation. At the end, this approach allows the circumferential dimension to be included in the analysis through the focus on each tube of every panel. Furthermore, it allows to obtain the incident and absorbed heat flow rates variations along the path taken by the HTF.

2. Development of the external receiver model

The model is based on the steady-state energy balance of the heat flow components entering and leaving one single CV. The main outputs are the temperature of the HTF leaving the receiver ($T_{HTF_{out}}$) and the external surface temperature of the receiver (T_{surf}^{cv}).

The core of the model is presented in Figure 1, where a cross section of a single tube is illustrated. The absorbed heat flow rate by the tube´s surface ($\dot{Q}_{inc} * \alpha_{paint}$) is the result of the incident heat flow rate ($\dot{Q}_{inc}$) subtracted by the reflected fraction of it to the surroundings ($\dot{Q}_{ref}$). The heat flow rate that is absorbed by the HTF ($\dot{Q}_{abs}^{net}$) is then obtained by subtracting to the heat flow rate absorbed by the surface, the thermal losses through convection ($\dot{Q}_{conv}$) and radiation ($\dot{Q}_{rad}$). From this point, two resistances are present: resistance to conduction on the tube´s wall (R_{cond}) and resistance to convection from the tube´s inner surface to the HTF (R_{conv}^{int}). The surface temperature for each CV (T_{surf}^{cv}) is a function of these two resistances, on the absorbed heat flow rate by the HTF and on the average temperature of the HTF on the CV (T_{HTF}^{cv}). The energy balance is translated in equations 1.1 and 1.2:

$$\dot{Q}_{abs} = \dot{Q}_{inc} - \dot{Q}_{ref} = \dot{Q}_{inc} * \alpha_{paint} \quad (1.1)$$

$$\dot{Q}_{abs}^{net} = \dot{Q}_{abs} - \dot{Q}_{loss} = \dot{Q}_{abs} - (\dot{Q}_{conv} + \dot{Q}_{rad}) \quad (1.2)$$

The calculation algorithm behind the model is present in the scheme of Figure 2. The model starts by requiring the inputs to the user and then it sets a guess value for the average surface temperature of the entire receiver, which is corrected at the end once the new value is calculated. The sequence that follows

consists on repeatedly calling procedures and simultaneously checking if certain variables respond to certain statements. At this point it is important to define three variables: x (translates the panel), y (translates the tube in a certain panel) and z (translates the CV in a certain tube). The maximum value/upper limit is equal to the value set by the user for the number of panels (N_p), number of tubes per panel (n_t) and number of CV per tube (N_z), respectively. The actual calculations are done in the 'Procedure CV', where two guess values are defined for the final temperature of the HTF leaving the CV and the surface temperature of that same CV. Once the model calculates the heat flow rates absorbed and lost, the new values for these parameters are obtained. The two tolerances (TOL1 and TOL2) correspond to the difference between these initial guess values with the new values.

Concerning the assumptions and simplifications of the model: the tubes are assumed to be very close or touching each other, but since they are essentially the same, tube-to-tube conduction is neglected. It is considered that the wall behind the tubes acts as an insulant and as no part on the thermodynamic phenomena occurring. Conduction heat loss through the tube´s wall in the vertical and circumferential directions is not considered, since the amount of heat absorbed in the horizontal direction (from the surface to the HTF) is much more considerable and at least one order of magnitude higher (Rodriguez-Sanchez et al., 2014).

The incident heat flow rate is obtained by multiplying $\dot{p}_{inc}$ (the flux density taken from the flux map) by A_{inc} (the incident area of the CV – approximated as a flat surface). The flux map must be a file provided by the user in the *.lkt* format (lookup table recognized my EES).

The three-main mechanism for thermal losses from the central receiver are: reflection of the incident flux, convection to the ambient and radiation to the surroundings. Convection losses are calculated in accordance with the heat and mass transfer text books (Incropera et. al., 2002) as in equation 1.3. A_{cv} is the area of the CV, considered as half of a cylinder surface.

$$\dot{Q}_{conv} = \overline{h}_{mix} * A_{cv} * (T_{surf}^{cv} - T_{amb}) \qquad 1.3$$

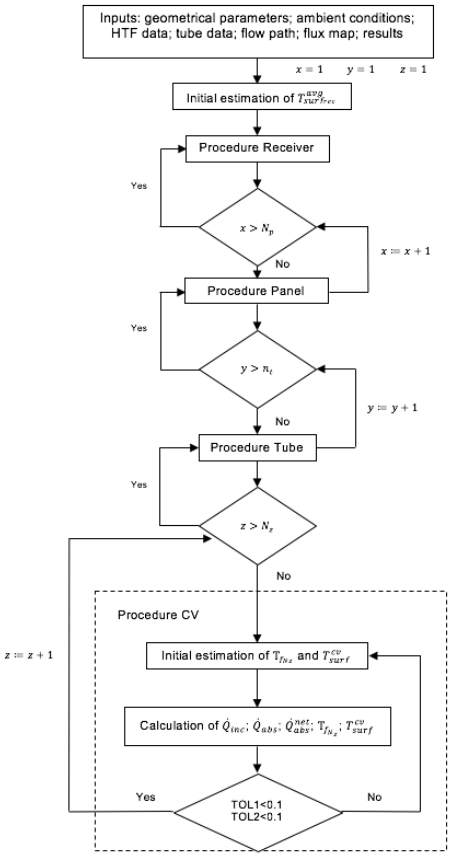

Figure 2 - Calculation algorithm of the model.

According to Siebers and Kraabel (Siebers & Kraabel, 1984), the composition of an external receiver, as a series of panels placed side by side around a cylinder, with each panel made up of thin tubes welded together, results in a rough receiver surface with roughness elements perpendicular to the wind - the vertical tubes themselves. The flow field around an element like this is complex and the traditional Nusselt number correlations for heat transfer from a cylinder that are provided in heat transfer text book or in EES internal functions that are adequate to small cylinder diameters, do not consider the surrounding context of these tubes. Hence, is more practical to calculate them for the entire receiver. To account for mixed convection the relationship of equation 1.4 is used to obtain the mix convective heat transfer coefficient, where $\overline{h}_{for}$ and $\overline{h}_{nat}$ represent the average

forced and natural convection coefficients, respectively.

$$\bar{h}_{mix} = (\bar{h}_{for}{}^{m} + \bar{h}_{nat}{}^{m})^{1/m} \quad 1.4$$

The Nusselt number for forced convection of air on a rough receiver surface is obtain through a set of correlations dependent on the specific surface roughness and on the Reynolds number, as in (Siebers & Kraabel, 1984). As for the Nusselt number for turbulent natural convection, a correlation for a vertical flat surface is used, since it is considered that the surface curvature in the horizontal direction has little effect on the natural heat transfer (Siebers & Kraabel, 1984).

Concerning the heat flow rate lost by radiation, it includes the net emitted radiation from the tube´s surface because of its temperature and the reflection of some of the incident flux density. On this context, we have radiation exchange between a small surface at temperature T_{surf}^{cv} and a much larger one at temperature $\mathrm{T_{surr}}$ that surrounds the smaller one. According to (Incropera et. al., 2002) the irradiation may be approximated by emission from a blackbody at $\mathrm{T_{surr}}$, in which case the irradiation is $G = \sigma {T_{surr}}^4$. If the surface is assumed to be one for which $\varepsilon = \alpha$ (grey surface) the net rate of radiation heat transfer from that surface, per unit area of the surface, is:

$$\dot{q}_{rad} = \varepsilon E_b - \alpha G = \varepsilon\sigma({T_{surf}}^4 - {T_{surr}}^4) \quad 1.5$$

Where E_b is the emissive power of a blackbody (calculated as $E_b = \sigma {T_{surf}}^4$), ε is the emissivity of the surface, α is the absorptivity of the surface, G is the irradiation and σ is the Stefan-Boltzmann constant. Hence, equation 1.5 expresses the difference between thermal energy that is released due to radiation emission and that which is gained due to radiation absorption per unit area of a surface (Incropera et. al., 2002).

The simplification of considering grey and diffuse surfaces is applied here, hence, emissivity and other properties are constant with the wavelength and the proprieties are also independent of the direction of the radiation.
The radiation losses represent the losses to the ground, sky and surrounding tubes (neglected since the tubes are considered to have similar surface temperatures). To account for these phenomena, the view factor (VF) parameter is used, which is a geometric quantity independent of the surface properties and temperature. Hence, the heat flow rate lost through radiation to the ground in a CV is calculated as follows (similar equation to the losses to the sky, with T_{sky} instead of T_{amb})

$$\dot{Q}_{rad}^{ground} = VF * A_{cv} * \varepsilon * \sigma * ({T_{surf}^{cv}}^4 - {T_{amb}}^4) \quad 1.6$$

The view factor was considered the same for radiation to the ambient and to the sky, as an approximation, and the value is obtained as in equation 1.7.

$$\mathrm{VF} = \frac{1 - \mathrm{VF_{tube}}}{2} \quad 1.7$$

Where $\mathrm{VF_{tube}}$ represents the VF of the radiation exchange between tubes, calculated through EES´s internal function (equation 1.8) that provides the VF from an infinitely long cylinder to a parallel infinitely long cylinder of identical diameter (Siegel & Howell, 2002). This function depends on the radius of the tubes and the distance between adjacent tubes, measured from the closest points on the cylinder´s surfaces.

$$\mathrm{VF_{tube}} = \frac{1}{\pi}(\sqrt{X^2 - 1} + \sin^{-1}\frac{1}{X} - X) \quad 1.8$$

$$X = 1 + \frac{s}{2 * r} \quad 1.9$$

At this point, the model calculates the final temperature of the HTF leaving the CV ($\mathrm{T}_{f_{N_z}}$) through equation 1.10, that derives from the general heat flow equation (Incropera et. al., 2002).

$$\mathrm{T}_{f_{N_z}} = \mathrm{T}_{i_{N_z}} + \frac{\dot{Q}_{abs}^{net}}{\dot{m}_{HTF} * c_{p_{HTF}}} \quad 1.10$$

Where $T_{i_{N_z}}$ is the initial temperature of the HTF, $\dot{m}_{HTF}$ is the mass flow rate of the HTF in each tube and $c_{p_{HTF}}$ the specific heat of the HTF obtained through EES internal functions for the specific HTF considered by the user. The final temperature of the HTF ($T_{f_{N_z}}$) and the temperature at the surface of the CV (T_{surf}^{cv}) are parameters to be calculated at the end of the procedure, but since they are also needed in the beginning of the calculations, there is the need to use guess values that later will be corrected through convergence between the guess and new value. The new value of $T_{surf_{cv}}$ is obtained through Equation 1.11, where R_{cond} depends on the tube´s thickness and on the conductivity of the material and R_{conv}^{int} depends on the convection coefficient of the inner surface of the tube (h_{int}) and the inside surface area.

$$T_{surf_{new}}^{cv} = T_{HTF}^{cv} + \dot{Q}_{abs}^{net} * (R_{cond} + R_{conv}^{int}) \quad 1.11$$

Regarding the thermopysical parameters of the HTF - density (ρ_{HTF}), viscosity (μ_{HTF}), specific heat ($c_{p_{HTF}}$) and conductivity (k_{HTF}) – they are obtained through EES internal functions, or provided by the user on a look table. And finally, once all the calculations are done for each CV, the thermal efficiency of the receiver is obtained through equation 1.12.

$$\eta_{therm} = \frac{\dot{Q}_{abs_{net}}^{total}}{\dot{Q}_{inc}^{total}} \quad 1.12$$

3. Comparison of the model with reference papers

Two simulations were made with the aim of comparing the main outputs with a reference paper, when using the same geometrical parameters, incident flux density on the receiver, HTF, inlet temperature, HTF mass flow rate and surrounding conditions. The goal was to verify the coherence of the model and its functionality. Also, for lack of resources, the model has not been simulated with experimental data.

Simulation I

The digital supplement of the work developed by Wagner (Wagner, 2008) provided the data needed for the first simulation. On Wagner´s model, the temperature of the HTF leaving the receiver ($T_{HTF_{out}}$) is a parameter set by the user and the HTF mass flow rate ($\dot{m}_{HTF}$) needed to achieve that value is calculated and results as an output. This data was used on the opposite way and for the model to be validated the $T_{HTF_{out}}$ had to be has close as possible to Wagner´s value. The receiver was simulated with 12 panels, with 104 tubes each, divided in 10 vertical CVs. The distribution of the incident flux density was created with the data available on Wagner´s electronic supplement accompanying his work and resulted on a matrix with 12 columns and 10 rows.

Table 1 presents a comparison between the outputs obtained through Wagner´s model and through this model with the respective absolute and relative differences. Regarding the heat flow rate lost, the main reason for the difference between the two models is the area of the CV used on the calculation of the convection and radiation losses. On the case of the developed model, it is considered the area of half the surface of the tube; on the case of Wagner´s model, it is used the same area as the one for the calculation of the incident radiative heat flow rate, which approximates the surface of the panel to a flat surface, not considering the existence of the tubes.

Table 1 – Comparison of the results with the reference paper for simulation I.

Parameter	Wagner	Developed model	Absolute difference	Relative Difference
$\dot{Q}_{abs}^{total}$ [W]	$7.547 * 10^7$	$7.547 * 10^7$	0.0	0.0%
$\dot{Q}_{abs_{net}}^{total}$ [W]	$7.211 * 10^7$	$7.027 * 10^7$	$-1.840 * 10^6$	-2.6%
$\dot{Q}_{loss}^{total}$ [W]	$3.360 * 10^6$	$5.204 * 10^6$	$1.844 * 10^6$	35.4%
$\dot{Q}_{loss_{conv}}^{total}$ [W]	$5.898 * 10^5$	$1.803 * 10^6$	$1.213 * 10^6$	67.3%
$\dot{Q}_{loss_{rad}}^{total}$ [W]	$2.771 * 10^6$	$3.401 * 10^6$	$6.300 * 10^5$	18.5%
$T_{HTF_{in}}$ [K]	565	565	0.0	-
$T_{HTF_{out}}$ [K]	838	830.9	-7.1	-
$\dot{m}_{HTF_{total}}$ [kg/s]	176.4	176.4	0.0	-
η_{total} [-]	0.90	0.88	-0.02	-

Besides the area of the CV considered, the difference between the convection losses (Figure 3) is also related with the temperatures that are used in equation 1.3. Wagner uses the difference between the surface temperature

(T_{surf}^{cv}) and the film temperature (T_{film}^{cv}); on the other hand, on the model it is used the difference between T_{surf}^{cv} and the ambient temperature (T_{amb}), as recommended by (Siebers & Kraabel, 1984).

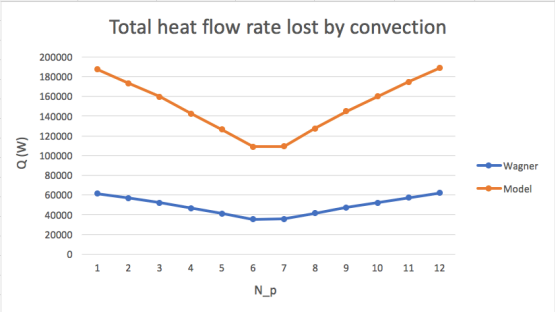

Figure 3 - Comparison of the total heat flow rate lost through convection on each panel for simulation I.

Other parameter influencing this gap in the surface temperature, which is, among other things, a function of the thermal resistances on the tube´s wall. Wagner uses an equation to calculate R_{cond} which is an approximation for a flat surface, implying that only half of the tube´s wall is conducting the heat to the HTF. Furthermore, Wagner uses an equation that was not understood or recognized from the data available on the literature. On the model, the equation used translates conduction through three quarters of the tube´s wall (considered a fair simplification on the context of a simplified model). Regarding R_{conv}^{int}, the same equation is used on the two models, once again with the difference between the areas: Wagner considers only half of the inside area of a tube, and, on the model, it is used three quarters of the inside area.

As for the differences on the radiation losses between the two models, they are a consequence of two things: the VF (which is 0.5 on Wagner´s case and 0.4 for the model) and the surface temperature. To confirm that this were the causes for the difference between the values of the convection losses and radiation losses, a simulation was made considering on the equation for the convection losses, T_{film}^{cv} instead of T_{amb} and a VF of 0.5. By doing so the difference between the convection losses changed from being initially 37.7% higher to only 1.7% lower on the model, and, for the radiation losses, they changed from 18.5% lower to only 2.5% lower.

Analyzing the comparison between the main parameters, namely absorbed and lost heat flow rates and final temperature of the HTF, it can be concluded that the model presented close results for the final temperature of the HTF (the goal of 838 K was almost reached with this model predicting a temperature of 7.1 K lower than Wagner´s model). The main reason for the divergence between the final temperature comes from the fact that the total heat flow rate lost on the receiver is 35.4% higher on the developed model, since the tube cylindrical surface area is considered, versus using a flat surface as an approximation (for calculating the thermal losses of an entire panel, which underestimates the real surface area exposed, as done by Wagner).

Simulation II

The paper taken as reference for the simulation II was the one developed by (Rodriguez-Sanchez et al., 2014). The two bi-dimensional simplified thermal models presented on the reference paper assume that the temperature at the surface of the tubes varies in axial and circumferential directions, as for the even more simplified model (SM) it is considered the same temperature to vary only in the axial direction. The goal of this paper was to understand if these models could reach similar results when comparing with a Computer Fluid Dynamics (CFD) model.

The main assumptions of the bi-dimensional thermal models are: to consider the tube´s surface as grey surface; the refractory wall behind the tubes is insulated with mineral wool (considered adiabatic) and the direction of the wind is north-south, since the effects are higher on the receiver on this direction. An important detail to refer at this point is the area of the CV that is used on each model. On the reference paper the tubes are separated by 2 mm distance, and since the refractory wall on the back of the tubes is taken into consideration for the thermal exchanges, it is assumed that the reference model considers the entire surface area of each tube during the calculations.

Concerning the incident flux density on the external receiver for simulation II, the data

presented on the reference paper was referent to a design point on the spring equinox-solar noon and, according to (Augsburger & Favrat, 2013), the flux radiation map on this moment is entirely symmetric with respect to the North-South axis for a Gemasolar-type heliostat field. Therefore, on the simulations presented on the reference paper, only one flow path was considered. The data available was referent to five different operational conditions (presented in Table 2), which varied on the wind velocity and/or HTF total mass flow rate. It was simulated a receiver with 9 panels with 24 tubes each and 13 CVs.

Table 2 – Operational conditions for simulation II.

	A	B	C	D	E
V_{wind} (m/s)	0.0	7.5	15.0	0.0	0.0
$\dot{m}_{HTF_{total}}$ (kg/s)	281.6	281.6	281.6	256.0	301.0

The difference between the results is presented on Table 3, for the total efficiency of the receiver, final HTF temperature and maximum surface temperature. Regarding the final temperature of the HTF, the best comparison was with the CFD model for the operational condition with no wind and higher HTF mass flow rate, case E. The best comparison for the total efficiency of the external receiver was also with the CFD results.

The model and the SM presented similar results, leading to a similar comparison with the CFD model: similar efficiencies and final HTF temperature, but different maximum surface temperatures. This difference between the surface temperatures is, most probably, because CFD models calculate local values of surface temperature, on the other hand, the SM and developed model calculate average values.

Regarding the maximum surface temperature on each panel, the values obtained were closer to the ones from the SM, as visible on Figure 4. This parameter diverged in a great deal when comparing with the CFD or bi-dimensional models. This shows the impact of calculating average temperatures instead of considering local values and of the number of CV (or grid divisions). On the CFD model, 439400 grid divisions are considered along the entire receiver, on the other hand, only 2808 are considered on the model. This difference in the level of detail affects directly the value that is considered as maximum for the surface temperature on each panel.

Table 3 – Absolute difference between the results of the developed model and the ones from the reference paper.

		A	B	C	D	E
Model vs. CFD	η_{total} [-]	0.04	0.04	0.04	0.04	0.03
	$T_{HTF_{out}}$ [K]	1.85	2.95	2.75	2.05	0.95
	$T^{cv}_{surf_{max}}$ [K]	-208.55	-196.45	-190.05	-199.95	-212.35
Model vs. HTM	η_{total} [-]	0.10	0.10	0.10	0.10	0.09
	$T_{HTF_{out}}$ [K]	18.95	20.35	20.45	20.85	17.75
	$T^{cv}_{surf_{max}}$ [K]	-227.65	-225.55	-224.55	-226.85	-228.25
Model vs. HHFM	η_{total} [-]	0.10	0.10	0.10	0.10	0.09
	$T_{HTF_{out}}$ [K]	18.95	20.45	16.55	20.95	17.85
	$T^{cv}_{surf_{max}}$ [K]	-227.65	-225.45	-224.45	-226.75	-228.15
Model vs. SM	η_{total} [-]	0.08	0.08	0.08	0.08	0.08
	$T_{HTF_{out}}$ [K]	14.35	15.45	15.25	15.25	13.55
	$T^{cv}_{surf_{max}}$ [K]	1.45	1.55	0.05	10.15	-4.35

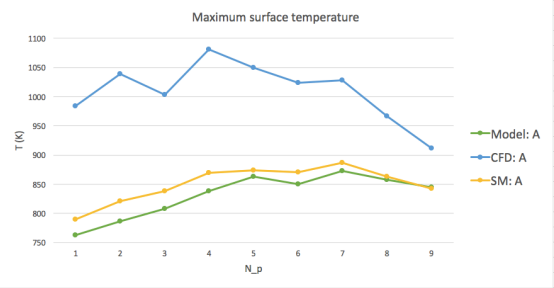

Figure 4 – Comparison of the maximum surface temperature for simulation II, case A.

Even though the final temperature of the HTF and the total efficiency of the receiver reached values which were very close to the CFD results, the surface temperature greatly differs between the two approaches, hence concluding that the model approach slightly overestimates the HTF temperature variation and underestimates the value of the external surface temperature. Further simulation with experimental data is needed to validate both parameters.

4. Application of the model

The model that was presented on this work implied a steady-state condition, hence representing a moment in time with the sun on a certain position - of azimuth and zenith - and with a certain DNI. Evaluating the thermodynamic phenomena considering quasi-steady conditions is a fair approximation of the

reality (for clear sky conditions), since the sun´s position and irradiance change relatively slow with time.

For the user to be able to simulate an entire day or even an entire year, the model must be applied successively for each moment in time. Hence, the model was simulated for an entire day with intervals of 30 minutes, with data for the DNI, zenith and azimuth solar angles, temperature and wind velocity obtained through the National Solar Radiation Database (NSRDB) (National Renewable Energy Laboratory (NREL), 2017). The transients during pre-heating mode and shutdown were neglected, as a simplification.

In the case of using the external receiver model to simulate an entire day, a different methodology is used for calculating the incident heat flow rate on each CV´s surface, through equation 1.13.

$$\dot{Q}_{inc} = DNI * A_{helio} * n_{helio} * \eta_{cv} \qquad 1.13$$

Where DNI is the Direct Normal Irradiation, A_{helio} is the area of a single heliostat, n_{helio} is the number of heliostats and η_{cv} is the efficiency of a single CV. The efficiency of a single CV is dependent on the sun´s position, namely zenith and solar angles, therefore a series of tables were created to calculate the efficiency of each CV. This was done running a series of simulations on the heliostat model, develop on Tonatiuh (Blanco, Amieva, & Mancilla, 2005) for a Gemasolar-type heliostat field, for different azimuth and zenith angles and obtaining the flux maps with the values of incident flux density on each CV. The number of CVs per panel can be defined by the user, for the example presented here it was defined that each panel had three CVs, hence considering that all the tubes of a panel received the same incident flux. Organizing the data, a series of tables resulted in which the efficiency is presented as a function of the zenith and azimuth angles for each CV.

The user should provide the lookup table with the hourly values for the DNI, solar angles, ambient temperature, wind velocity and ambient pressure for a maximum of 8760 hours, since EES commercial version doesn´t allow lookup tables with more than 8760 rows. Also, the efficiency values should be provided in separate lookup tables for each CV.

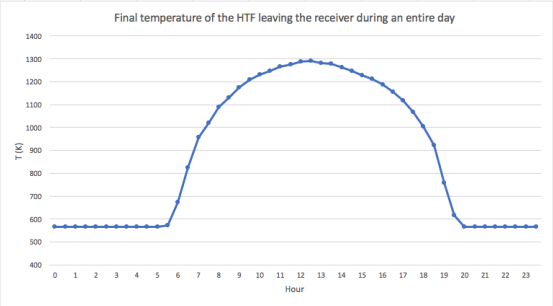

Figure 5 – Final temperature of the HTF leaving the receiver at each time step during an entire day.

Figure 5 presents the final temperature of the HTF leaving the receiver throughout the day. The shape is similar to the DNI variation. The high temperatures that are reached (above 1200 K, which is beyond the working temperatures for a nitrate molten salt) are due to the number of panels considered on this simulation, which was twelve. And the heliostat field is dimensioned to an external receiver with twenty-four panels, hence, the receiver is receiving higher flux densities on a smaller area, resulting on higher final temperatures of the HTF.

Figure 6 presents the average surface temperature of the entire receiver during a day. It is visible that the higher temperatures occur during the hours of higher DNI, on the top of the receiver. This is due to the higher efficiency of the CVs on that area on the value of incident flux that is incident on that same area.

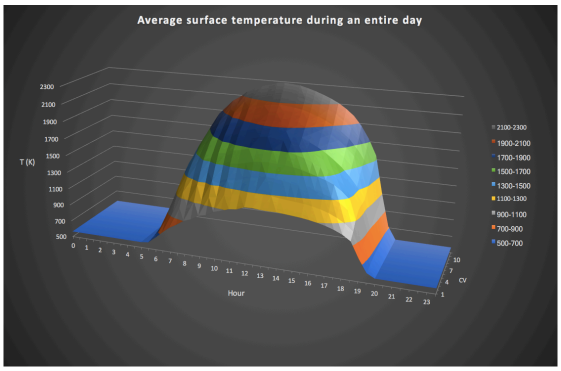

Figure 6 – Average surface temperatures on the receiver during an entire day.

5. Conclusion

The purpose of this work was to develop and simulate a model of a Solar Power Tower (SPT) external receiver that used molten salt as Heat Transfer Fluid (HTF), starting from the equations found in the literature that described the main thermodynamic phenomena and implementing them on a computational algorithm using the commercial software Engineering Equation Solver (EES). The model was based on a simplified approach, hence considering variation of the temperature of external receiver´s surface only on the vertical direction, tube-to-tube conduction was neglected and the conduction of heat is unidimensional, hence, from the receiver´s surface to the HTF. Even though the model calculates all the parameters for each single control volume, the convection coefficients were calculated as average values for the entire receiver, since it was the best approach found in literature considering the nature of the flow around the external receiver.

The two simulations that were made to compare the results of the model with other models established on the literature led to different conclusions. On the first simulation, comparing with the work done by Michael Wagner (Wagner, 2008), it was concluded that the main reason for the difference between the outputs derived from the area of the control volume considered for the calculation of the convection and radiation losses: Wagner considered the approximation for a flat surface, therefore neglecting the existence of the tubes; on the developed model, the thermal losses are calculated using the real area of the tubes exposed to the surroundings (the area of the surface of a cylinder). Furthermore, two other factors influenced the difference between the total heat flow rate lost: the temperatures used when calculating the convection losses and the view factors considered when calculating the radiation losses.

On the second simulation, the available data for comparison forced a more general analysis of the results. The final temperature of the HTF obtained with the model was closer to the Computer Fluid Dynamics (CFD) results than to the bi-dimensional or simplified models, which was considered a positive result, since CFD models are considered to have the highest precision (even though that without experimental data the results cannot be considered as real values). No comparison was made concerning the losses that occur on the receiver´s surface, due to the lack of data. The average temperature at the surface of each panel was closer to the Standard Model (SM) results and varied in a great deal with the CFD results. Hence, using a simplified approach that calculates average values of temperature instead of local ones, results on a good prediction of the final temperature of the HTF and of the total receiver's efficiency, but on an inaccurate prediction of the external surface temperature, resulting in an underestimate of the maximum surface temperature. Moreover, since the model undervalues the external surface temperature, it does the same regarding the internal surface temperature (the critical point of design to predict problems like the corrosion rate of the tubes or the HTF decomposition), which means that it is not the most adequate model to perform a receiver design (namely the material of the tubes, tube thickness or tube diameter, for instance). Nevertheless, the model correctly estimates the temperature variations of the HTF, standing as a viable tool for studying the energy performance of an external receiver, which was the main goal of this work. Also, it is important to have tools for the pre-design of these power plants, which requires the energy performance simulation of the different components of the system (namely the external receiver).

Adding to the external receiver model, the heliostat field model developed in Tonatiuh (Blanco et al., 2005) was useful to create the tables of the efficiency of each CV for different azimuth and zenith angles, on a receiver with twelve panels, needed for calculating the incident heat flow rate when simulating the model during an entire day. The application of the model to different operating conditions adds an extra feature, allowing the user to study the variations of the heat flow rate absorbed by the HTF and the final temperatures leaving the receiver for different hours of a day.

The main advantages of the developed model for the external receiver are: the fact that it is a simplified approach, hence a useful tool for users that wish to simulate the temperature variation of the HTF without a lot of complexity, computational tools and time; the user´s interface gives flexibility for different molten salts and flow paths, allowing the user to study the impact of choosing one or another; the code for the model is written in EES, hence it is a relatively simple set of equations and functions that can be easily understood, and the output parameters are available at the end of each simulation in separated files, which allows the user to analyze the variations of the HTF temperature or of heat flow rates along the flow path taken by the HTF.

6. Future Work

Further work on the model for the external receiver can start from the validation with experimental data, especially to verify the external surface temperature of the receiver, since this parameter had different values for both comparisons made on chapter 3. Also, the external receiver model lacks the implementation of transients that include the thermal capacity of the HTF during pre-heating and shutdown periods, hence, further work can be done on this subject. At last, optimization of the model to reduce the computational time can still be done, especially for simulating a day, or even an entire year.

7. References

Augsburger, G., & Favrat, D. (2013). Modelling of the receiver transient flux distribution due to cloud passages on a solar tower thermal power plant. *Solar Energy*, *87*(1), 42–52. http://doi.org/10.1016/j.solener.2012.10.010

Blanco, M. J., Amieva, J. M., & Mancilla, A. (2005). The Tonatiuh Software Development Project: An open source approach to the simulation of solar concentrating systems. *Proceedings of the ASME Computers and Information in Engineering Division*, 157–164. http://doi.org/10.1115/IMECE2005-81859

EASAC. (2011). *Concentrating solar power : its potential contribution to a sustainable energy future*. German Academy of Sciences.

Incropera, Dewitt, Bergman, & Lavine. (2002). *Fundamentals of Heat and Mass Transfer* (6th ed.). New York. J. Wiley.

National Renewable Energy Laboratory (NREL). (2017). *National Solar Radiation Database*. Retrieved March 21, 2017, from NREL: https://nsrdb.nrel.gov/nsrdb-viewer

Neises, T., & Wagner, M. J. (2012). Simulation of Direct Steam Power Tower Concentrated Solar Plant. *ASME 2012 6th International Conference on Energy Sustainability, Parts A and B*, 499–507. http://doi.org/10.1115/ES2012-91364

Reilly, Hugh E.; Kolb, G. J. (2001). *An Evaluation of Molten-Salt Power Towers Including results of the Solar Two Project*. (No. SAND2001-3674). Sandia National Labs., Albuquerque, NM (US); Sandia National Labs., Livermore, CA (US)

Rodriguez-Sanchez, M. R., Marugan-Cruz, C., Acosta-Iborra, A., & Santana, D. (2014). Comparison of simplified heat transfer models and CFD simulations for molten salt external receiver. *Applied Thermal Engineering*, *73*(1), 991–1003. http://doi.org/10.1016/j.applthermaleng.2014.08.072

Siebers, D. L., & Kraabel, J. S. (1984). *Estimating Convective Energy Losses From Solar Central Receivers*. (No. SAND-84-8717). Sandia National Labs., Livermore, CA (USA).

Siegel, R., & Howell, J. (2002). *Thermal radiation heat transfer* (Vol. 4).

Stine, W., & Geyer, M. (2001). *Power From The Sun.* www.powerfromthesun.net

Wagner, M. J. (2008). Thesis MSc. Simulation and Predictive Performance Modeling of Utility-Scale Central Receiver System Power Plants, 259. Retrieved from http://sel.me.wisc.edu/publications/theses/wagner08.zip

Yao, Y., Hu, Y., & Gao, S. (2015). Heliostat field layout methodology in central receiver systems based on efficiency-related distribution. *Solar Energy*, *117*, 114–124. http://doi.org/10.1016/j.solener.2015.04.029

Yunus A. Cengel, A. J. (2011). *Heat and Mass Transfer: Fundamentals & Applications.* McGraw-Hill.